• Clinical Research •

Change in choroid thickness and vascularity index associated with accommodation and aberration after small-incision lenticule extraction

Dan Cheng[1], Yi−Lin Qiao[1], Xue−Ying Zhu[1], Kai−Ming Ruan[1], Heng−Li Lian[1], Mei−Xiao Shen[1], Shu−Lin Wang[2], Li−Jun Shen[1,3], Yu−Feng Ye[1]

[1]National Clinical Research Center for Ocular Diseases, Eye Hospital, Wenzhou Medical University, Wenzhou 325035, Zhejiang Province, China

[2]Department of Ophthalmology, Henan Provincial People's Hospital, Zhengzhou 325035, Henan Province, China

[3]Department of Ophthalmology, Zhejiang Provincial People's Hospital, Hangzhou 310000, Zhejiang Province, China

Co-first authors: Dan Cheng and Yi-Lin Qiao

Correspondence to: Yu-Feng Ye. The Affiliated Eye Hospital of Wenzhou Medical University, 618 Fengqi East Road, Hangzhou 310000, Zhejiang Province, China. yyf0571@mail.eye.ac.cn

Abstract

● **AIM:** To explore choroidal thickness (CT) and choroidal vascularity index (CVI) changes around the macula and optic nerve head (ONH) using swept-source optical coherence tomography (SS-OCT) after small-incision lenticule extraction (SMILE) and evaluate their associations with accommodation and aberrations.

● **METHODS:** Participants were divided into more myopic group (43 eyes) and less myopic group (33 eyes) according to refractive error. SS-OCT, negative relative accommodation (NRA), and positive relative accommodation (PRA) were analyzed before and 1d, 1wk, and 1mo postoperatively. Root mean square higher-order aberrations (RMS HOAs), spherical aberrations (SAs), and coma were compared preoperative, 1wk, and 1mo postoperatively.

● **RESULTS:** After surgery, RMS (0.29±0.26) and Coma (0.16±0.19) all increased. In the more myopic group, central and T1 macular CT (247.58±63.81 and 276.45±62.52 µm) increased. NRA (0.41±0.51) and PRA (0.10±1.30) decreased, and SAs (0.21±0.21) increased. In the less myopic group, all regional and mean macular CT increased. NRA was correlated with mean and inferior CTs and mean ONH CVI. SE was correlated with macular CT, CVI, and ONH CT. Mean macular and ONH CTs were associated with RMS HOA, SA, and coma. Macular T2 CT was a significant predictor of SA. Macular T2 and N1 CT were correlated with coma.

● **CONCLUSION:** More variations in accommodation and aberrations and fewer choroid thickens on macular and ONH are found in more myopic eyes after SMILE. Choroidal values are associated with accommodation and aberrations during SMILE. Choroid parameters on SS-OCT varies in eyes with different refractive errors after SMILE and has an association with accommodation and visual quality.

● **KEYWORDS:** swept-source optical coherence tomography; small-incision lenticule extraction; choroid thickness; accommodation; aberration

INTRODUCTION

Small-incision lenticule extraction (SMILE) is the most recent development in refractive surgery and has gained worldwide acceptance as a safe and accurate surgical technique[1-2]. After first reported in 2011, SMILE received the United States Food and Drug Administration approval in 2016 and was reported to correct myopia of up to −10.00 D with astigmatism of up to −5.00 D[3-4].

Posterior segment complications after refractive surgery have been studied more widely, in addition to corneal, anterior segment injury and wound healings[5-12]. Anteroposterior traction caused by the suction process as well as laser effect during the procedure may result in posterior effects, such as posterior vitreous detachment, retinal detachment, macular holes, and choroidal neovascularization. However, limited information is available regarding posterior changes following femtosecond laser irradiation, although previous studies have extensively studied the influence of excimer lasers[6-7,11-12].

Moreover, the precise effects of SMILE on the choroid have not yet been determined.

Swept-source optical coherence tomography (SS-OCT) utilizes a tunable swept laser and enables a faster scan rate, thus enabling the incorporation of longer wavelengths than conventional spectral-domain OCT[13]. With better visualization of the choroid and choroidal-scleral boundary due to deeper penetration and lower scattering from the retinal pigment epithelium, SS-OCT has become more frequently used in routine clinical practice. In addition, choroidal thickness (CT) and choroidal vascularity index (CVI) were considered reliable innovative imaging OCT-based choroidal parameters[14]. Our previous work quantified CT and CVI changes around the macula and optic disc head (ONH) in eyes with myopia and glaucoma and precisely reported their variation during axial elongation and excision[15].

Knowledge of choroidal changes that occur in myopia after refractive surgery is limited. Li et al[7] used SD-OCT to measure CT, while Yalçınkaya[11] only investigated choroidal microvascularity until the postoperative 7th day. Recent studies have shown that choroid had a good correlation with progressive myopia[14,16-17]. Moreover, as part of the accommodative apparatus of the eye, the choroid might be associated with accommodation change[18] and further corneal aberrations, especially higher-order aberrations (HOAs)[19-20]. However, no studies have precisely quantified CT and CVI variations around the macula and ONH after SMILE using SS-OCT and investigated the association between these changes and negative relative accommodation (NRA), positive relative accommodation (PRA), and aberrations.

The current study aimed to characterize the choroid in the macula and ONH following SMILE using SS-OCT. We also investigated the relationship between choroidal changes and accommodation and aberrations.

PARTICIPANTS AND METHODS

Ethical Approval This prospective study was approved by the Ethics Committee of the Affiliated Eye Hospital of Wenzhou Medical University (H2022-008-K-08-01) and adhered to the tenets of the Declaration of Helsinki. All the participants provided written informed consent.

Participants The inclusion criteria were as follows: age ≥18y, myopia from −1.00 to −10.00 D, with up to −3.00 D cylinder, manifest spherical equivalent of up to −11.50 D, stable refraction over the past year (change by <0.25 D), and corrected distance visual acuity (CDVA) of 20/20 or better. Exclusion criteria were central corneal thickness of <480 μm, calculated residual stromal thickness of <280 μm, abnormal corneal topographic features, clinically significant dry eye, eyelid or corneal diseases, previous intraocular or corneal surgery, glaucoma or preoperative intraocular pressure (IOP)

of >21 mm Hg, diabetes, hypertension, pregnancy, and breastfeeding. Preoperative and postoperative measurements included refractive error assessment (sphere, cylinder, and axis), NRA, PRA, pupil size (Atlas, Carl Zeiss Meditec, Jena, Germany), slit-lamp examination, fundus examination, corneal topography (Pentacam HR type 70900, Oculus, Wetzlar, Germany), IOP (non-contact tonometer, Topcon, Japan), axial length (IOL Master 700; Carl Zeiss Meditec, Jena, Germany), and SS-OCT examination (VG200S; SVision Imaging, Henan, China). Postoperative examinations were scheduled at 1d, 1wk, and 1mo postoperatively. IOP measurement and Pentacam were avoided 1d after surgery to avoid patient discomfort. Patients had both eyes evaluated for surgical assessment, and the data output all eyes that underwent surgery was enrolled in the analysis. All enrolled eyes were grouped into the more myopic group (spherical equivalent, SE≤-4.50 D) and the less myopic group (SE>-4.50 D).

On measuring NRA and PRA with correction, 20/20 on a high-contrast near chart at 40 cm was set as the fixation target. To test NRA and PRA, we changed the accommodation using minus and plus lenses, respectively. The lenses were added binocularly in 0.25 D steps until the first slight sustained blur appeared. We recorded the total number of plus lenses added for NRA testing and minus lenses for PRA testing. NRA was assessed before PRA.

The Pentacam HR device uses a rotating Scheimpflug camera to obtain elevation data and form a three-dimensional reconstruction of the corneal structure. Root mean square higher-order aberrations (RMS HOAs), spherical aberrations (SAs), and coma were automatically converted from the corneal elevation profile (Figure 1).

Surgical Procedure All surgeries were performed by the same surgeon (Ye YF). SMILE was performed using a 500-kHz VisuMax femtosecond laser system (Carl Zeiss Meditec, Jena, Germany) with a pulse energy of 140 nJ. When patients laid down, head position was readjusted by cross-assistance before the standard SMILE procedure[21]. After femtosecond laser application was completed, the lenticule was dissected and completely extracted. The lenticule diameter (optical zone) was set between 6.00 and 6.80 mm, and the cap thickness was 110–120 μm. A single-sided cut of 2 mm length was created at the 110° position of the cornea. After the femtosecond laser cutting procedure was completed, the suction was switched off, followed by lenticule extraction through the side-cut. After surgery, topical 0.5% levofloxacin (Cravit; Santen, Inc., Japan) eye drops were applied four times daily for 1wk, and 0.1% fluorometholone (Allergan, Inc., USA) eye drops and non-preserved artificial tears were administered four times daily for the first week, then sequentially reduced to three, two, and one time every 1wk.
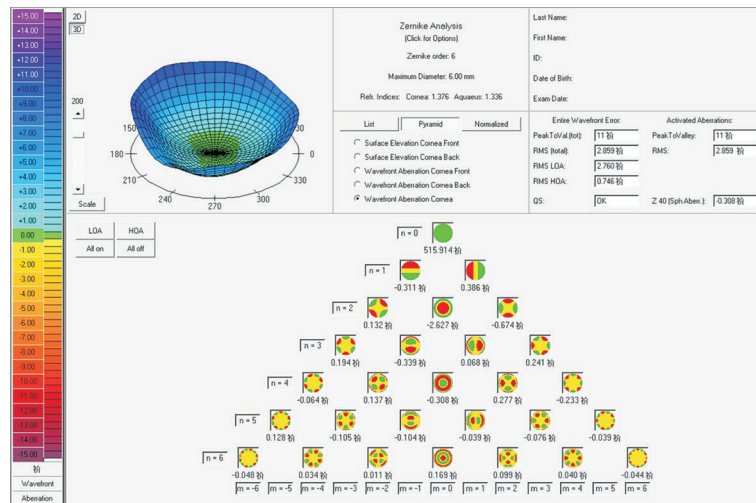
Figure 1 Zernike analysis using the Pentacam HR device to achieve RMS higher-order aberration (HOA), spherical aberration (SA), and coma automatically RMS: Root mean square.
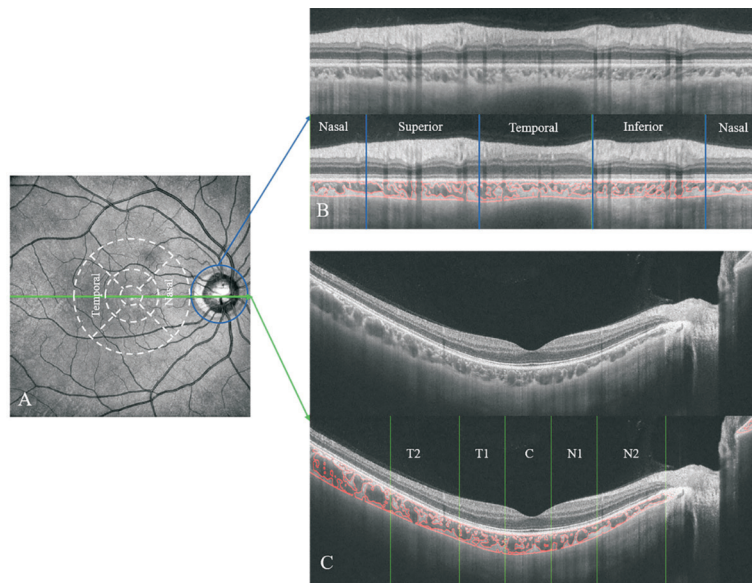

Figure 2 Measurement of CT and CVI around the macula and ONH A: Infrared fundus photography of the retina including the macula and ONH. B: CT and CVI around the ONH were measured along the outer edge of a 3.4-mm-diameter circle centered on the ONH using MATLAB. The ONH zone was divided into four parts, including superior, inferior, nasal, and temporal. C: CT and CVI around the macula were measured along the horizontal scan passing through the fovea and calculated into five parts. T1 and T2: Temporal region extended from the inner diameter of 1 and 3 mm to the outer diameter of 3 and 6 mm, respectively. C: A diameter of 1 mm centered on fovea. N1 and N2: Nasal region extends from the inner diameter of 1 and 3 mm to the outer diameter of 3 and 6 mm, respectively. CT: Choroidal thickness; CVI: Choroidal vascularity index; ONH: Optic nerve head.

SS-OCT Image Analysis To limit the effect of the circadian rhythm on choroidal parameters, SS-OCT images were collected between 9.00 *a.m.* and 12.00 *a.m.* A cutoff signal strength index value of ≥6 was used as the inclusion criterion. A horizontal OCT line scan encompassing the fovea was obtained (Figure 2A). ONH OCT was performed using 4.5 mm×4.5 mm scans. CVI and CT were assessed using a circle scan of 3.4-mm diameter centered on the ONH (Figure 2B) and the horizontal scan centered on the macula (Figure 2C), respectively. After semiautomatic choroidal segmentation using a custom-built algorithm in MATLAB R2017a

(MathWorks, Natick, MA, USA)[16,22], two trained examiners (Ruan KM and Qiao YL) manually modified the segments. Further, each picture was binarized to demarcate the luminal area and stromal area. The mean macular CT, total choroidal area, luminal area, and stromal area were estimated after image processing, and the size was adjusted to account for changes in magnification between the eyes due to differing axial length. The ratio of luminal area to total choroidal area was used to calculate CVI.

The macular zone was split into three concentric rings with diameters of 1 (central fovea, C), 3, and 6 mm. The central

Table 1 Characteristics of eyes that underwent SMILE

Characteristics	More myopic group	Less myopic group	P
Eyes	43	33	Not applicable
Sphere error (D)	-5.25 (-6.25, -4.75)	-2.80±0.85	<0.001
Cylinder error (D)	-0.75 (-1.50, -0.50)	-0.50 (-1.13, 0.00)	0.040
Spherical equivalent (D)	-6.00 (-7.00, -5.00)	-3.12±0.84	<0.001
CDVA, logMAR	0.00 (0.00, 0.00)	0.00 (0.00, 0.00)	0.599
CCT (µm)	537.14±26.93	526.30±22.47	0.106
IOP corrected (mm Hg)	13.84±1.67	14.47±3.07	0.362
Ablating depth (µm)	122.95±16.57	77.82±17.19	<0.001
Residual thickness of stromal bed (µm)	407 (394, 427)	447.58±27.23	<0.001

CDVA: Corrected distance visual acuity; IOP: Intraocular pressure; CCT: Central corneal thickness.

region centered on the fovea had a diameter of 1 mm. T1 and T2 within the temporal regions extended from an inner diameter of 1 and 3 mm to an outer diameter of 3 and 6 mm, respectively. N1 and N2 were defined as the nasal region extending from an inner diameter of 1 and 3 mm to an outer diameter of 3 and 6 mm, respectively. The ONH zone was split into four parts: temporal, superior, inferior, and nasal regions. CT and CVI were calculated along the line within each region of the macula and ONH.

Statistical Analysis Statistical analysis was performed using the SPSS statistical software version 26 (SPSS 157 Inc., Chicago, IL, USA). The Shapiro-Wilk test was used to evaluate the normality of data. The generalized estimating equation with Bonferroni's post-hoc test was used to compare the difference of more myopic and less myopic group between preoperative and postoperative values. Linear regression analyses were used to investigate the influence of CT and CVI on NRA, PRA, SE, and aberrations. Statistical significance was set at a P value of <0.05.

RESULTS

Demographic Data A total of 76 eyes from 39 patients were included (Table 1) in this study. The mean age of the patients was 29.26±6.77y. Twenty-three patients were women (58.97%) and 16 (41.03%) were men. The mean manifest SE was −4.86±1.93 D and 0.25 (0, 0.50) D before and 1mo after surgery respectively (P<0.001).

Before the SMILE surgery, sphere error, cylinder error, and SE of the more myopic group were significantly less than the less myopic group (P<0.001, P=0.040, and P<0.001, respectively).

At 1mo postoperatively, 73 (96%) eyes had uncorrected distance visual acuity (UDVA) of 20/20 or better (Figure 3). Eleven (14%) eyes lost one line of CDVA after surgery. The linear regression model of attempted SE versus achieved SE achieved an R^2 of 0.951. SE predictability was within ±0.5 D in 83.78% of eyes. Astigmatism predictability was within -0.50 D in 96% of eyes.

Change in Choroidal Parameters, NRA, PRA, and Corneal Aberrations Following SMILE Table 2 depicted the variations in SE, NRA, PRA, corneal aberration, CT, and CVI around the macula and ONH before and 1mo after the SMILE procedure of the more myopic and less myopic group, respectively. After surgery, RMS HOAs (0.29±0.26) and coma (0.16±0.19) increased significantly in both groups (P<0.001). In the more myopic group, NRA (0.41±0.51) decreased at 1mo and PRA (0.10±1.30) decreased at 1d (P=0.013 and P<0.001, respectively), and SA (0.21±0.21) increased at both time points (P<0.001).

In the more myopic group, a significant increase occurred in the macular CT in the central (P=0.010) and T1 (P=0.001) region at 1wk and 1mo after surgery. There was significant change in macular N2 CVI (P=0.043) and ONH temporal CVI (P=0.009). In the less myopic group, the macular CT in all regions increased after surgery (P<0.05). Except the ONH temporal CT, there were significant changes in all ONH CTs after surgery. Macular mean and central CVI showed significant changes after the surgery.

Correlation of Choroidal Parameters with NRA, PRA, SE, and Corneal Aberrations Table 3 showed the relationships between CT, CVI, NRA, PRA, and SE. We adopted NRA, PRA and SE as explanatory variables in the regression models. According to the univariate and multivariate analyses, NRA was correlated with mean (β=−0.003, P=0.017) and inferior (β=−0.004, P=0.040) CTs on ONH and mean CVI on ONH (β=−0.026, P=0.019). SE was correlated with macular CT (β=0.004, P<0.001) and CVI (β=0.047, P=0.018) and ONH CT (β=0.003, P=0.043).

Table 4 depicted the associations between CT, CVI, RMS HOA, SA, and coma. Corneal aberration parameters were adopted as explanatory variables in different regression models. Mean CTs around macular and ONH were associated with RMS HOA (β=−0.001, P=0.004; β=−0.001, P=0.034), SA (β=−0.001, P<0.001; β=−0.001, P=0.043) and coma (β=−0.001, P=0.016; β=−0.001, P=0.023). Macular CT in

Table 2 Evaluation of choroidal parameters, NRA, PRA and corneal aberrations following SMILE

Parameters	Pre-operation	Post-operation			P
		1-day	1-week	1-month	
More myopic group					
SE	-6.00 (-7.00, -5.00)	0.06 (-0.13, 0.25)[a]	0.25 (0.00, 0.38)[a]	0.18±0.32[a]	<0.001
NRA	3.00 (2.50, 3.00)	2.63 (2.44, 3.00)	2.50 (2.00, 3.25)	2.43±0.54[a]	0.013
PRA	-3.50 (-5.50, -2.75)	-2.75 (-3.50, -1.50)[a]	-3.00 (-4.13, -2.44)	-4.00±1.33	<0.001
RMS HOA	0.35±0.07	Not applicable	0.63 (0.52, 0.82)[a]	0.70 (0.53, 0.87)[a]	<0.001
SA	0.18±0.08	Not applicable	0.31 (0.19, 0.45)[a]	0.36 (0.28, 0.47)[a]	<0.001
Coma	0.14±0.06	Not applicable	0.27 (0.15, 0.38)[a]	0.29 (0.19, 0.48)[a]	<0.001
Macula					
CT					
Mean	222.42±45.04	224.59±48.14	229.29±50.03	228.31±47.18	0.153
T2	260.67±50.08	257.34 (232.16, 317.96)	264.18±57.83	266.55±57.13	0.305
T1	262.04±58.13	269.15±63.89	273.15±63.38[a]	276.45±62.52[a]	0.001
C	235.66±55.65	241.02±64.16	247.612±66.07[a]	247.58±63.81[a]	0.010
N1	203.95±52.93	204.13±52.68	212.26±52.81	207.70±51.15	0.176
N2	155.04 (127.17, 189.90)	155.55 (125.08, 182.30)	164.35±43.08	152.24 (130.45, 179.76)	0.357
CVI					
Mean	58.82 (56.14, 61.19)	58.00±4.90	59.15±3.27	58.89±4.38	0.141
T2	58.08±5.22	59.21 (54.85, 62.19)	58.65±4.48	58.31±5.44	0.678
T1	58.59±4.78	58.23±4.81	59.15±4.68	57.84±4.69	0.139
C	58.50±5.33	57.76±5.96	59.47±5.61	58.84±5.65	0.177
N1	60.58±7.18	60.90±8.16	61.96±5.76	62.09±6.78	0.053
N2	57.02±6.82	56.38±8.04	57.87±7.03	59.18±7.98	0.043
ONH					
CT					
Mean	175.30±38.26	172.82±37.43	178.09±39.62	174.35±34.67	0.430
T	144.49±36.99	141.76±38.24	149.39±42.23	145.91±38.01	0.057
S	195.94±48.25	194.72±42.75	198.60±42.92	197.70±41.59	0.658
N	59.21 (54.85, 62.19)	185.05 (165.59, 218.48)	198.89±52.30	190.82 (169.56, 221.60)	0.730
I	161.97±31.89	159.62±31.92	155.73 (143.52, 188.52)	158.91±31.98	0.380
CVI					
Mean	49.50±5.40	49.48 (44.53, 51.78)	49.64±5.39	49.27±5.60	0.120
T	46.10±6.99	44.03 (40.02, 50.02)[a]	46.32±8.12	45.77 (42.21, 51.41)	0.009
S	52.39±6.33	51.97 (46.53, 55.51)	52.10±6.38	51.97±5.50	0.267
N	49.86±6.4	49.46 (43.39, 51.48)	49.97±5.72	49.27±7.18	0.299
I	49.13±5.08	48.32 (43.70, 53.39)	49.66±5.23	49.56±5.75	0.168
Less myopic group					
SE	-3.12±0.84	0.00 (-0.13, 0.25)[a]	0.26±0.29[a]	0.30±0.36[a]	<0.001
NRA	2.75 (1.75, 3.00)	2.50 (2.00, 2.75)	2.75 (2.00, 3.00)	2.50 (1.81, 2.94)	0.144
PRA	-2.75 (-3.75, -2.00)	-3.10±1.43	-3.75 (-4.50, -3.00)	-3.13 (-5.25, -2.50)	0.133
RMS HOA	0.34 (0.31, 0.40)	Not applicable	0.42 (0.36, 0.48)[a]	0.51±0.14[a]	<0.001
SA	0.19±0.07	Not applicable	0.17 (0.11, 0.25)	0.19 (0.12, 0.30)	0.150
Coma	0.14±0.06	Not applicable	0.15 (0.10, 0.24)	0.20 (0.15, 0.27)[a]	<0.001
Macula					
CT					
Mean	294.17±63.07	298.53±62.53	313.17±65.27[a]	308.48±59.84[a]	<0.001
T2	332.60±55.30	334.77±63.98	345.61±61.98	346.53±61.96	0.013
T1	341.38±72.04	348.96±72.14	362.64±75.08	362.08±71.13[a]	0.001
C	323.73±77.87	329.30±72.87	348.87±78.33[a]	341.47±70.77	<0.001

Table 2 Evaluation of choroidal parameters, NRA, PRA and corneal aberrations following SMILE (continued)

Parameters	Pre-operation	Post-operation			P
		1-day	1-week	1-month	
N1	285.81±78.79	292.14±73.73	309.63±81.67[a]	299.15±72.56	<0.001
N2	210.21±73.94	212.47±76.45	226.41±79.80[a]	218.99±73.72	<0.001
CVI					
Mean	60.05±3.70	59.98±3.08	59.69±2.94	60.69±2.88	0.001
T2	59.01±4.04	59.59±4.28	59.61±3.42	60.24±3.29	0.235
T1	61.05 (57.86, 63.90)	60.89±3.94	60.73±4.20	61.69±3.66	0.240
C	60.54±4.97	59.25±4.48	59.30±4.71	60.72±4.40	0.004
N1	61.31±6.22	60.87±5.72	60.22±5.60	61.10±5.99	0.257
N2	59.07±6.54	59.16±7.58	58.17±6.43	59.68±6.00	0.286
ONH					
CT					
Mean	205.40 (153.12, 269.93)	207.14±65.07	212.31±60.33	203.49±58.37	0.008
T	171.33 (126.90, 255.28)	178.75 (123.92, 255.65)	195.98±70.23	179.88 (135.98, 244.66)	0.496
S	232.82±68.95	224.02±69.82	237.19±69.42	235.41±69.07	0.008
N	215.32±68.83	217.04±65.54	227.67±63.96	209.85±63.25	0.003
I	180.68±54.86	191.28±63.55	188.82±52.24	166.88 (139.18, 200.68)	0.001
CVI					
Mean	50.40±6.25	50.30±5.35	50.61±6.02	50.46±5.90	0.908
T	46.83±7.62	49.59 (42.42, 51.72)	48.02±6.79	47.28±7.15	0.143
S	52.57±6.20	53.50±5.32	52.63±5.16	51.83±5.260	0.185
N	51.98±8.09	50.82±6.96	50.95±8.11	50.95±6.69	0.163
I	50.09±7.28	49.84±6.41	50.62±7.10	51.87±7.91	0.086

NRA: Negative relative accommodation; PRA: Positive relative accommodation; RMS HOA: The root-mean-square values of higher-order aberrations; SA: Spherical aberration; ONH: Optic nerve head; CT: Choroidal thickness; CVI: Choroidal vascularity index; C: Central; T: Temporal; S: Superior; N: Nasal; I: Inferior; SMILE: Small-incision lenticule extraction. [a]Significant differences between pre-operative and post-operative values.
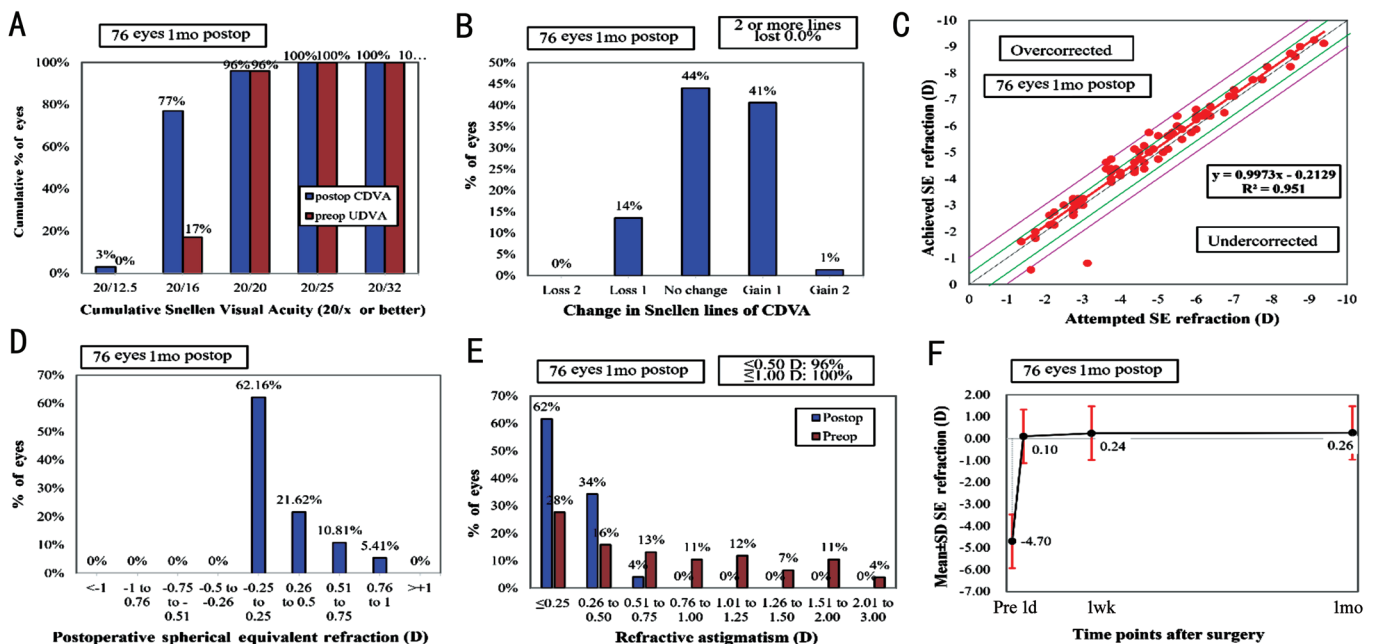

Figure 3 Six standard graphs for corneal refractive surgery.

the T2 region was a significant predictor of SA (β=−0.001, P=0.037). Macular CT in the T2 (β=−0.005, P=0.019) and N1 (β=0.005, P=0.026) regions were also correlated with coma.

DISCUSSION

In the current study, there was a more trend in macular and ONH CT increasing in the less myopic eyes, while the NRA

Table 3 Linear regression analysis to determine the correlations between ocular parameters and NRA, PRA, SE

Parameters	NRA						PRA						SE					
	Univariate analysis			Multivariate analysis			Univariate analysis			Multivariate analysis			Univariate analysis			Multivariate analysis		
	β	P	95%CI	β	P	95%CI	β	P	95%CI	β	P	95%CI	β	P	95%CI	β	P	95%CI
SE	-0.137	0.048	-0.272 to -0.001	-0.108	0.098	-0.236 to 0.020	0.086	0.505	-0.167 to 0.338				-	-	-	-	-	-
UDVA, logMAR	-0.161	0.723	-1.053 to 0.731				-0.175	0.816	-1.653 to 1.303				-5.396	<0.001	-6.594 to -4.198	-5.199	<0.001	-6.380 to -4.019
CDVA, logMAR	-1.461	0.121	-3.307 to 0.386				-1.391	0.464	-5.115 to 2.333				-0.876	0.472	-3.263 to 1.511			
Macula																		
CT																		
Mean[a]	-0.002	0.085	-0.005 to 0.000				0.001	0.700	-0.004 to 0.006				0.004	<0.001	0.002 to 0.005			
T2	-0.001	0.229	-0.004 to 0.001				0.001	0.683	-0.004 to 0.005				0.004	<0.001	0.002 to 0.005	0.000	0.960	-0.004 to 0.004
T1	-0.002	0.091	-0.004 to 0.000				0.002	0.274	-0.002 to 0.006				0.003	<0.001	0.002 to 0.005	0.000	0.898	-0.005 to 0.005
C	-0.002	0.086	-0.004 to 0.000				0.002	0.315	-0.002 to 0.006				0.003	<0.001	0.002 to 0.004	0.000	0.837	-0.004 to 0.005
N1	-0.002	0.095	-0.004 to 0.000				0.000	0.846	-0.004 to 0.005				0.003	<0.001	0.002 to 0.004	0.001	0.695	-0.003 to 0.005
N2	-0.002	0.051	-0.004 to 0.000				-0.001	0.605	-0.006 to 0.004				0.003	0.003	0.001 to 0.005	0.000	0.904	-0.004 to 0.003
CVI																		
Mean[a]	-0.009	0.536	-0.036 to 0.019				0.020	0.499	-0.038 to 0.079				0.047	0.018	0.008 to 0.085			
T2	0.000	0.978	-0.018 to 0.018				0.023	0.231	-0.015 to 0.061				0.034	0.026	0.004 to 0.063	0.002	0.858	-0.021 to 0.025
T1	-0.023	0.059	-0.047 to 0.001				0.035	0.140	-0.011 to 0.082				0.032	0.046	0.001 to 0.064	0.008	0.557	-0.018 to 0.034
C	-0.002	0.796	-0.018 to 0.014				0.001	0.955	-0.040 to 0.042				0.023	0.049	0.000 to 0.047	0.000	0.989	-0.021 to 0.022
N1	0.004	0.652	-0.013 to 0.021				0.010	0.583	-0.025 to 0.044				0.017	0.110	-0.004 to 0.037			
N2	-0.005	0.424	-0.018 to 0.007				-0.003	0.873	-0.041 to 0.035				0.003	0.714	-0.014 to 0.020			
ONH																		
CT																		
Mean[a]	-0.003	0.017	-0.006 to -0.001				-0.002	0.521	-0.008 to 0.004				0.003	0.043	0.000 to 0.005			
T	-0.003	0.006	-0.005 to -0.001	0.000	0.845	-0.002 to 0.003	-0.002	0.458	-0.008 to 0.004				0.003	0.002	0.001 to 0.005	0.000	0.922	-0.003 to 0.003
S	-0.002	0.059	-0.004 to 0.000				-0.003	0.233	-0.008 to 0.002				0.002	0.036	0.000 to 0.005	0.001	0.465	-0.002 to 0.003
N	-0.002	0.147	-0.005 to 0.001				-0.001	0.836	-0.005 to 0.004				0.001	0.303	-0.001 to 0.004			
I	-0.004	0.003	-0.007 to -0.001	-0.004	0.040	-0.007 to 0.000	-0.001	0.822	-0.007 to 0.006				0.002	0.099	0.000 to 0.005			
CVI																		
Mean[a]	-0.026	0.019	-0.047 to -0.004				-0.002	0.932	-0.055 to 0.050				-0.005	0.623	-0.025 to 0.015			
T	-0.025	0.003	-0.041 to -0.008	-0.018	0.137	-0.042 to 0.006	-0.004	0.845	-0.045 to 0.037				-0.003	0.776	-0.021 to 0.016			
S	-0.022	0.020	-0.040 to -0.004	0.005	0.656	-0.018 to 0.028	-0.008	0.716	-0.054 to 0.037				-0.008	0.356	-0.025 to 0.009			
N	-0.013	0.158	-0.032 to 0.005				0.005	0.802	-0.036 to 0.046				-0.002	0.852	-0.019 to 0.016			
I	-0.022	0.010	-0.040 to -0.005	-0.006	0.490	-0.022 to 0.010	0.000	0.984	-0.046 to 0.045				-0.001	0.884	-0.017 to 0.015			

SE: Spherical equivalent; CDVA: Corrected distance visual acuity; UDVA: Uncorrected distance visual acuity; ONH: Optic nerve head; CT: Choroidal thickness; CVI: Choroidal vascularity index; C: Central; T: Temporal; S: Superior; N: Nasal; I: Inferior; -: Not applicable; NRA: Negative relative accommodation; PRA: Positive relative accommodation. [a]To avoid repeated measurements and multicollinearity, the mean was not included in the multivariate analysis.

Table 4 Linear regression analysis to determine the correlations between ocular parameters and aberrations

Parameters	RMS HOA						SA						Coma					
	Univariate analysis			Multivariate analysis			Univariate analysis			Multivariate analysis			Univariate analysis			Multivariate analysis		
	β	P	95%CI	β	P	95%CI	β	P	95%CI	β	P	95%CI	β	P	95%CI	β	P	95%CI
SE	0.001	0.939	-0.012 to 0.013				0.003	0.597	-0.008 to 0.014				-0.001	0.914	-0.011 to 0.010			
UDVA, logMAR	0.035	0.553	-0.080 to 0.149				-0.062	0.404	-0.206 to 0.083				0.023	0.546	-0.051 to 0.097			
CDVA, logMAR	0.598	0.083	-0.079 to 1.275				0.087	0.843	-0.779 to 0.953				0.195	0.502	-0.374 to 0.764			
Macula																		
CT																		
Mean[a]	-0.001	0.004	-0.002 to 0.000				-0.001	<0.001	-0.001 to 0.000				-0.001	0.016	-0.001 to 0.000			
T2	-0.001	0.008	-0.002 to 0.000				-0.001	<0.001	-0.001 to 0.000	-0.001	0.037	-0.001 to 0.000	-0.001	0.038	-0.001 to 0.000	-0.005	0.019	-0.009 to -0.001
T1	-0.001	0.010	-0.002 to 0.000				-0.001	<0.001	-0.001 to 0.000	0.000	0.579	-0.001 to 0.001	-0.001	0.051	-0.001 to 0.000			
C	-0.001	0.004	-0.002 to 0.000				-0.001	<0.001	-0.001 to 0.000	-0.001	0.114	-0.003 to 0.000	-0.001	0.027	-0.001 to 0.000	-0.004	0.121	-0.010 to 0.001
N1	-0.001	0.002	-0.002 to 0.000				-0.001	0.001	-0.001 to 0.000	0.001	0.405	-0.001 to 0.002	-0.001	0.010	-0.001 to 0.000	0.005	0.026	0.001 to 0.010
N2	-0.001	0.005	-0.001 to 0.000				0.000	0.046	-0.001 to 0.000	0.000	0.647	-0.001 to 0.001	-0.001	0.007	-0.001 to 0.000	-0.003	0.272	-0.010 to 0.003
CVI																		
Mean[a]	-0.012	0.078	-0.025 to 0.001				-0.009	0.012	-0.017 to -0.002				-0.006	0.200	-0.016 to 0.003			
T2	-0.008	0.018	-0.014 to -0.001				-0.003	0.250	-0.009 to 0.002				-0.004	0.096	-0.009 to 0.001			
T1	-0.008	0.005	-0.013 to -0.002				-0.006	0.006	-0.010 to -0.002	-0.002	0.332	-0.007 to 0.002	-0.004	0.117	-0.008 to 0.001			
C	-0.003	0.263	-0.009 to 0.003				-0.003	0.239	-0.007 to 0.002				-0.003	0.232	-0.007 to 0.002			
N1	-0.001	0.734	-0.007 to 0.005				-0.004	0.052	-0.007 to 0.000				0.000	0.875	-0.004 to 0.005			
N2	-0.004	0.339	-0.013 to 0.005				-0.004	0.103	-0.009 to 0.001				-0.003	0.272	-0.009 to 0.003			
ONH																		
CT																		
Mean[a]	-0.001	0.034	-0.002 to 0.000				-0.001	0.043	-0.001 to 0.000	0.000	0.864	-0.001 to 0.001	-0.001	0.023	-0.001 to 0.000			
T	-0.001	0.008	-0.001 to 0.000				-0.001	0.014	-0.001 to 0.000				-0.001	0.014	-0.001 to 0.000	0.000	0.555	0.000 to 0.001
S	-0.001	0.112	-0.001 to 0.000				-0.001	0.065	-0.001 to 0.000				0.000	0.088	-0.001 to 0.000			
N	-0.001	0.077	-0.001 to 0.000				0.000	0.118	-0.001 to 0.000				-0.001	0.040	-0.001 to 0.000	0.000	0.498	-0.001 to 0.000
I	-0.001	0.021	-0.002 to 0.000				-0.001	0.065	-0.001 to 0.000				-0.001	0.009	-0.001 to 0.000	-0.001	0.126	-0.002 to 0.000
CVI																		
Mean[a]	-0.005	0.379	-0.015 to 0.006				-0.002	0.579	-0.009 to 0.005				-0.005	0.206	-0.012 to 0.003			
T	-0.002	0.589	-0.009 to 0.005				-0.001	0.619	-0.006 to 0.004				-0.003	0.308	-0.007 to 0.002			
S	-0.004	0.347	-0.013 to 0.005				-0.002	0.537	-0.008 to 0.004				-0.003	0.288	-0.009 to 0.003			
N	-0.006	0.225	-0.015 to 0.004				-0.001	0.640	-0.007 to 0.004				-0.005	0.080	-0.012 to 0.001			
I	-0.003	0.485	-0.010 to 0.005				-0.002	0.407	-0.007 to 0.003				-0.002	0.396	-0.008 to 0.003			

CDVA: Corrected distance visual acuity; UDVA: Uncorrected distance visual acuity; RMS HOA: The root-mean-square values of higher-order aberrations; SA: Spherical aberration; ONH: Optic nerve head; CT: Choroidal thickness; CVI: Choroidal vascularity index; C: Central; T: temporal; S: Superior; N: nasal; I: Inferior; -: Not applicable; CI: Confidence interval. [a]To avoid repeated measurements and multicollinearity, the mean was not included in the multivariate analysis.

and PRA decreased, and corneal aberration increased more significantly in the more myopic eyes. NRA was associated with ONH CT and CVI. We further found that mean macular and ONH CTs were the significant predictors of SE and corneal aberrations, including RMS HOA, SA and coma. Macular regional CTs were the significant predictor of SA and coma. Macular mean CVI was also associated with SA.

Using SS-OCT, we precisely demonstrated a transient variation in CT and CVI after SMILE. An increasing trend in CTs was observed after surgery, especially in the less myopic eyes. We speculate this can be attributed to several mechanisms. During surgery, the application of a suction ring leads to a rapid increase in IOP, changes in the shape of the anterior segment, displacement of the lens, and compression and decompression of the posterior segment[5]. The anteroposterior traction or compression potentially leads to decrease in lens thickness and an increase in vitreous distance, especially in young patients aged <40y, whose posterior capsule of the lens strongly adheres to the anterior hyaloid. The decrease in lens thickness is accompanied by a forward movement of the anterior hyaloid, causing traction at the vitreous base, and posterior pole, and further conducting the power vector to the retina or choroid. Some researchers theorized that laser energy may cause disturbances in the ocular microstructure and biomechanics, although minimal but still present[23]. We speculate that choroidal structural changes may be explained by the increased accommodation demand in the early postoperative period because of overcorrection[7]. As the ciliary muscle is inserted into regions of the choroid, contraction of the ciliary muscle may be transmitted to the choroid. On the other hand, rather than CT fluctuation in the macular and ONH regions, few CVI variations were found in the current study, demonstrating a limited fluctuations of choroidal vasculature. Moreover, most regions of macular CT were thickened at 1mo after SMILE, especially in the less myopic group. Linear regression analysis showed a strong positive correlation between all regions of macular CT and SE. The same trend of changes was also shown in the previous study[24]. There was a common understanding that the more myopic eyes possess thinner retinal and CT owing to the elongation of ocular axial length[25], which might leads to relative small changes in CTs in more myopic eyes after surgery. However, a previous study speculated that the thickening of CTs following myopic excimer laser surgery improves patients' visual function to a certain extent[7]. Patients with high myopia suffered more severe corneal aberrations and less significant CT changes postoperatively, warranting tailored monitoring and management strategies. Recent studies have shifted the focus of myopic research to the choroid, which is an important initial factor in myopia[17,26]. We firstly characterized choroidal

structural and vasculature alterations before and after SMILE precisely using the SS-OCT system.

We found a trend of decreasing in NRA and PRA at 1d after surgery was observed. Further, the variations of NRA and PRA after surgery were more significant in the more myopic group. First, we propose that the application of the suction ring beneath the limbus leads to circular traction on the sclera, adjacent ciliary body, and zonula ciliaris, resulting in traction on the equatorial region of the lens, causing a decrease in lens thickness[5]. We speculate that this effect on the ocular accommodative apparatus, including the ciliary body, ciliary muscle, and choroid, may be preserved in the early postoperative period, especially 1d after surgery, leading to a decrease in NRA, PRA, and CT. Second, the early blurred vision due to increased HOAs, corneal edema, and cavity after surgery may lead to decreased accommodative stimulation[27], resulting in decreased NRA and PRA. To decrease the impact of refractive error on statistical analysis, we set two groups according to the severity of myopia. Our result showed that the stability ability in the more myopic eyes might be weaker.

Linear regression analysis showed that ONH CT and CVI were associated with NRA, while no parameter was associated with PRA. Accommodation is a mechanism that affects visual clarity and binocular vision[28]. The NRA and PRA have two different nervous pathways and measures the maximum ability to stimulate accommodation while maintaining binocular single vision[29-30]. A previous study reported that NRA was the highest in hyperopic participants[29]. Our result confirmed the contribution of the structural choroid to the accommodation system. In addition, the decrease in the PRA following SMILE was more obvious than that of NRA, which was accordance with the previous study that a direct relationship was found only between accommodation facilities and NRA, as PRA was proven to decrease with age. The detection of disorders of the accommodation and choroid may explain the mechanism of asthenopia after SMILE in the clinic.

We found the correlation between aberrations and CT and CVI values. Our study was similar to previous studies in which HOAs increased after SMILE[31-32]. Previous studies on the effects of HOAs on accommodation have reported that both SA and coma change with accommodation[19,33]. However, no study has associated HOAs with the choroid after SMILE. HOAs contribute to visual quality after refractive surgery. We speculate that following visual recovery after surgery, the visual information being transferred through neurotransmitters from the retina to the choroid may lead to microstructural changes in the choroid[34]. As the choroid is composed of numerous large blood vessels[35], macular CVI may be a predictor of RMS HOAs.

The current study had several limitations. First, this study only included a horizontal OCT scan line passing through the fovea to analyze CT. However, previous studies have demonstrated that choroidal thinning is most prominent in the temporal parafoveal zone under high accommodative stimuli using OCT[18]. Second, the eyes at postoperative 1d had a slightly lower signal strength score than those at other times. Therefore, we used a value of 6 as the cutoff signal strength index and further excluded images with obvious artifacts. Third, the postoperative follow-up was only continued until 1mo after the surgery. Longer follow-up period would be needed in future study. In conclusion, we demonstrated more variations in NRA, PRA and corneal aberrations, and less CT thickens around the macular and ONH in more myopic eyes after SMILE using SS-OCT. NRA was mainly correlated with ONH CT and CVI values. Aberrations were mainly correlated with macular CTs. Our results suggest that the SS-OCT system with functional analysis has the potential to become a technique for the evaluation of ocular changes and to understand the mechanisms underlying the various changes during accommodation and visual recovery after refractive surgery.

ACKNOWLEDGEMENTS

Conflicts of Interest: Cheng D, None; **Qiao YL,** None; **Zhu XY,** None; **Ruan KM,** None; **Lian HL,** None; **Shen MX,** None; **Wang SL,** None; **Shen LJ,** None; **Ye YF,** None.

REFERENCES

1 Dishler JG, Slade S, Seifert S, *et al*. Small-incision lenticule extraction (SMILE) for the correction of myopia with astigmatism: outcomes of the United States food and drug administration premarket approval clinical trial. *Ophthalmology* 2020;127(8):1020-1034.

2 Blum M, Täubig K, Gruhn C, *et al*. Five-year results of small incision lenticule extraction (ReLEx SMILE). *Br J Ophthalmol* 2016;100(9): 1192-1195.

3 Taneri S, Kießler S, Rost A, *et al*. Small-incision lenticule extraction for the correction of myopic astigmatism. *J Cataract Refract Surg* 2019;45(1):62-71.

4 Chan TCY, Wang Y, Ng ALK, *et al*. Vector analysis of high (≥3 diopters) astigmatism correction using small-incision lenticule extraction and laser *in situ* keratomileusis. *J Cataract Refract Surg* 2018;44(7):802-810.

5 Mirshahi A, Kohnen T. Effect of microkeratome suction during LASIK on ocular structures. *Ophthalmology* 2005;112(4):645-649.

6 Zhang Y, Lan JQ, Cao D, *et al*. Microvascular changes in macula and optic nerve head after femtosecond laser-assisted LASIK: an optical coherence tomography angiography study. *BMC Ophthalmol* 2020;20(1):107.

7 Li M, Cheng H, Yuan Y, *et al*. Change in choroidal thickness and the relationship with accommodation following myopic excimer laser surgery. *Eye* (*Lond*) 2016;30(7):972-978.

8 Ma Ruiz-Moreno J, Alió JL. Incidence of retinal disease following refractive surgery in 9, 239 eyes. *J Refract Surg* 2003;19(5):534-547.

9 Singhvi A, Dutta M, Sharma N, *et al*. Bilateral serous macular detachment following laser *in situ* keratomileusis. *Am J Ophthalmol* 2004;138(6):1069-1071.

10 Bailey CS. Choroidal neovascularization after LASIK in a patient with low myopia. *J Cataract Refract Surg* 2006;32(1):4.

11 Yalçınkaya G, Yıldız BK, Çakır İ, *et al*. Evaluation of peripapillary - macular microvascularity and choroidal vascularity index after refractive surgery. *Photodiagn Photodyn Ther* 2022;37:102714.

12 Chen YW, Liao HP, Sun Y, *et al*. Short-term changes in the anterior segment and retina after small incision lenticule extraction. *BMC Ophthalmol* 2020;20(1):397.

13 Laíns I, Wang JC, Cui Y, *et al*. Retinal applications of swept source optical coherence tomography (OCT) and optical coherence tomography angiography (OCTA). *Prog Retin Eye Res* 2021;84:100951.

14 Agrawal R, Ding JB, Sen P, *et al*. Exploring choroidal angioarchitecture in health and disease using choroidal vascularity index. *Prog Retin Eye Res* 2020;77:100829.

15 Cheng D, Ruan KM, Wu MH, *et al*. Characteristics of the optic nerve head in myopic eyes using swept-source optical coherence tomography. *Invest Ophthalmol Vis Sci* 2022;63(6):20.

16 Wu H, Zhang GY, Shen MX, *et al*. Assessment of choroidal vascularity and choriocapillaris blood perfusion in anisomyopic adults by SS-OCT/OCTA. *Invest Ophthalmol Vis Sci* 2021;62(1):8.

17 Xiong SY, He XG, Zhang B, *et al*. Changes in choroidal thickness varied by age and refraction in children and adolescents: a 1-year longitudinal study. *Am J Ophthalmol* 2020;213:46-56.

18 Logan NS, Radhakrishnan H, Cruickshank FE, *et al*. IMI accommodation and binocular vision in myopia development and progression. *Invest Ophthalmol Vis Sci* 2021;62(5):4.

19 Gyldenkerne A, Aagaard N, Jakobsen M, *et al*. Changes in accommodative function following small-incision lenticule extraction for high myopia. *PLoS One* 2020;15(12):e0244602.

20 Del Águila-Carrasco AJ, Kruger PB, Lara F, *et al*. Aberrations and accommodation. *Clin Exp Optom* 2020;103(1):95-103.

21 Li FF, Yang YZ, Bao FJ, *et al*. Comparison of astigmatic correction with and without cross-axis alignment during small incision lenticule extraction. *J Refract Surg* 2022;38(10):624-631.

22 Agrawal R, Gupta P, Tan KA, *et al*. Choroidal vascularity index as a measure of vascular status of the choroid: Measurements in healthy eyes from a population-based study. *Sci Rep* 2016;6:21090.

23 Marshall J. The 2014 bowman lecture-bowman's and bruch's: a tale of two membranes during the laser revolution. *Eye* (*Lond*) 2015;29(1): 46-64.

24 Zhao PF, Zhou YH, Zhang J, *et al*. Analysis of macular and retinal nerve fiber layer thickness in children with refractory amblyopia after femtosecond laser-assisted laser *in situ* keratomileusis. *Chin Med J* 2017;130(18):2234-2240.

25 Fujiwara T, Imamura Y, Margolis R, *et al*. Enhanced depth imaging optical coherence tomography of the choroid in highly myopic eyes. *Am J Ophthalmol* 2009;148(3):445-450.

26 Jin PY, Zou HD, Xu X, *et al*. Longitudinal changes in choroidal and retinal thicknesses in children with myopic shift. *Retina* 2019;39(6):1091-1099.

27 Siedlecki J, Schmelter V, Schworm B, *et al*. Corneal wavefront aberrations and subjective quality of vision after small incision lenticule extraction. *Acta Ophthalmol* 2020;98(7):e907-e913.

28 Hoffman DM, Girshick AR, Akeley K, *et al*. Vergence-accommodation conflicts hinder visual performance and cause visual fatigue. *J Vis* 2008;8(3):33.1-3330.

29 Yekta A, Hashemi H, Khabazkhoob M, *et al*. The distribution of negative and positive relative accommodation and their relationship with binocular and refractive indices in a young population. *J Curr Ophthalmol* 2017;29(3):204-209.

30 McDougal DH, Gamlin PD. Autonomic control of the eye. *Compr Physiol* 2015;5(1):439-473.

31 Zhao XH, Zhang L, Ma JN, *et al*. Comparison of wavefront-guided femtosecond LASIK and optimized SMILE for correction of moderate-to-high astigmatism. *J Refract Surg* 2021;37(3):166-173.

32 Hamilton DR, Chen AC, Chen AC, *et al*. Comparison of early visual outcomes after low-energy SMILE, high-energy SMILE, and LASIK for myopia and myopic astigmatism in the United States. *J Cataract Refract Surg* 2021;47(1):18-26.

33 Hughes RPJ, Read SA, Collins MJ, *et al*. Higher order aberrations and retinal image quality during short-term accommodation in children. *Vision Res* 2021;188:74-84.

34 Seko Y, Tanaka Y, Tokoro T. Apomorphine inhibits the growth-stimulating effect of retinal pigment epithelium on scleral cells *in vitro*. *Cell Biochem Funct* 1997;15(3):191-196.

35 Nickla DL, Wallman J. The multifunctional choroid. *Prog Retin Eye Res* 2010;29(2):144-168.